A numerical investigation of the gain profile of a PbSe quantum dot/Raman hybrid amplifier

O. MAHRAN[a], N. El-NOHY[a], H. IBRAHIM[a,b,*]
aFaculty of Science, Physics Department, Alexandria University, Mohrambeik 21511, Alexandria, Egypt
bFaculty of Engineering, Basic Engineering Science Department, International Academy of Engineering and Media Science, Cairo, Egypt

A PbSe quantum dot (PbSe-QD)/Raman hybrid optical fiber amplifier is proposed. The gain profile and its dependence on the constituent amplifiers length and pumping power is studied and compared to a PbSe-QD only and Raman only amplifiers. The values of fiber lengths and pumping power under study for Raman are 5-30 km and 50-400 mW respectively, while for the PbSe-QD are 0-44 cm and 50-300 mW, respectively. By changing the size and distribution of the PbSe quantum dots, pumping scheme and wavelengths of the Raman fiber, this hybrid amplifier would have the advantage of being highly tunable.

1. Introduction

Optical amplifiers play an important role in Dense Wavelength Division Multiplexing (DWDM) and Coarse Wavelength Division Multiplexing (CWDM) network communication systems. Different types of optical amplifiers have been used through the past decade, including the use of rare-earth ion doped fibers in which the most common used is Er^{+3} doped fiber amplifier (EDFA) [1], [2]. Co-doping Ytterbium (Yb) ions with Er^{+3} ions causes indirect pumping of Er^{+3} ions that leads to a reduction of the up-conversion rate of Er^{+3} by decreasing the Er^{+3} clusters. Similar work was also investigated by L. Goldberg and J. Koplow [3] where they obtained a 47 dB gain for a small signal and a 4.7 dB noise figure from a 3.5 m Er/Yb co-doped fiber. Other doping rare-earth ions include Nd^{+3} [4], Tm^{+3} [5], Ho^{+3} [6] and Pr^{+3} [7]. Another method of optical amplification is the distributed Raman optical amplifiers where optical amplification is provided through the process of Stokes scattering. Gain [8],[9] could be provided at any desired wavelength by tunning the pumping wavelength and the gain bandwidth could be broadened by increasing the number of pumps. This could be achieved either through co-propagating pumping scheme, counter-propagating pumping scheme or the bidirectional pumping scheme. Several commercial Raman amplifiers of interest in this report include the SMF, Allwave, TrueWave RS, LEAF, CORNING DSF and Corning NZDSF [10]. Recent interest has also arisen in the optimization of the gain characteristics of Raman amplifiers through numerical simulation and several optimization algorithms [11]–[16]. Due to limitations in further improvements on rare-earth ions doped amplifiers and rapid development in nanocrystal material science, interest has increased in the use of quantum amplifiers as dopants which are zero-dimensional nano-crystals such as

CdSe [17], CdTe [18], PbS [19] and PbSe [20] which possess some desirable emission spectra in wavelengths spanning 465-2340 nm. Small changes in the size of these nanoparticles lead to variations in the transition wavelengths and their spectral width. There have been several reports on quantum-dot fiber amplifiers (QDFA) in recent decades, in which Cheng et al. [21] used a three-level system to investigate the gain characteristics of PbSe through numerical simulation and concluded that the proposed QDFA can function on a long-wavelength band that have a wider bandwidth and lower noise than of the EDFAs. Cheng et al. [22] also proposed a multi-quantum dot amplifier (MQDA) and its numerical simulation produced a flatter gain. Bahrampour et al. [23] proposed an inhomogeneous model for PbSe (QDFA). Interest in hybrid optical amplifiers also ensued from the need of further development on optical amplifiers. These are amplifiers that have combinations of EDFA or EDFA co-doped with Yetterbium ions. Mahran et al. [24] studied the effect of bending loss on an EDFA/Raman hybrid amplifier. Mahran et al. [25] also studied the gain and noise figure of Er^{+3} co-doped with Yb^{+3}/ Raman fiber hybrid amplifier. Singh et al. [26] used a genetic algorithm to optimize the performance of a EDFA/Raman hybrid amplifier. Obaid et al. [27] suggested through numerical simulation a novel flat-gain L-band Raman/Er-Yb co-doped fiber hybrid optical amplifier. Obaid et al. [28] also studied the gain, noise figures and Q-factor of several configuration for hybrid amplifiers. Yusoff et al. [29] demonstrated a remotely pumped L-band erbium-doped fiber amplifier for long-haul transmission system. As mentioned earlier, the literature over hybrid amplifiers has mainly focused on EDFA/Raman and EDFA-related hybrid amplifiers whose gain characteristics are restricted by the photoluminescence and the absorbance properties of the EDFA amplifier. In this report, to the best of our

knowledge, we have studied for the first time the gain of a PbSe-QD/Raman amplifier for several modern commercial Raman amplifiers. We also study the effect of changing several parameters on the gain of such amplifiers. These parameters are the length of the fiber and the pumping power for both Raman and PbSe-QD amplifiers. By changing the size of the doped PbSe QDs and the pumping

scheme, this proposed amplifier would have the advantage of having highly tunable gain characteristics. In this report, we describe our theoretical model and the equations used in the simulation in section 2, our results graphically with further discussions in section 3, finally, our conclusions in section 4.
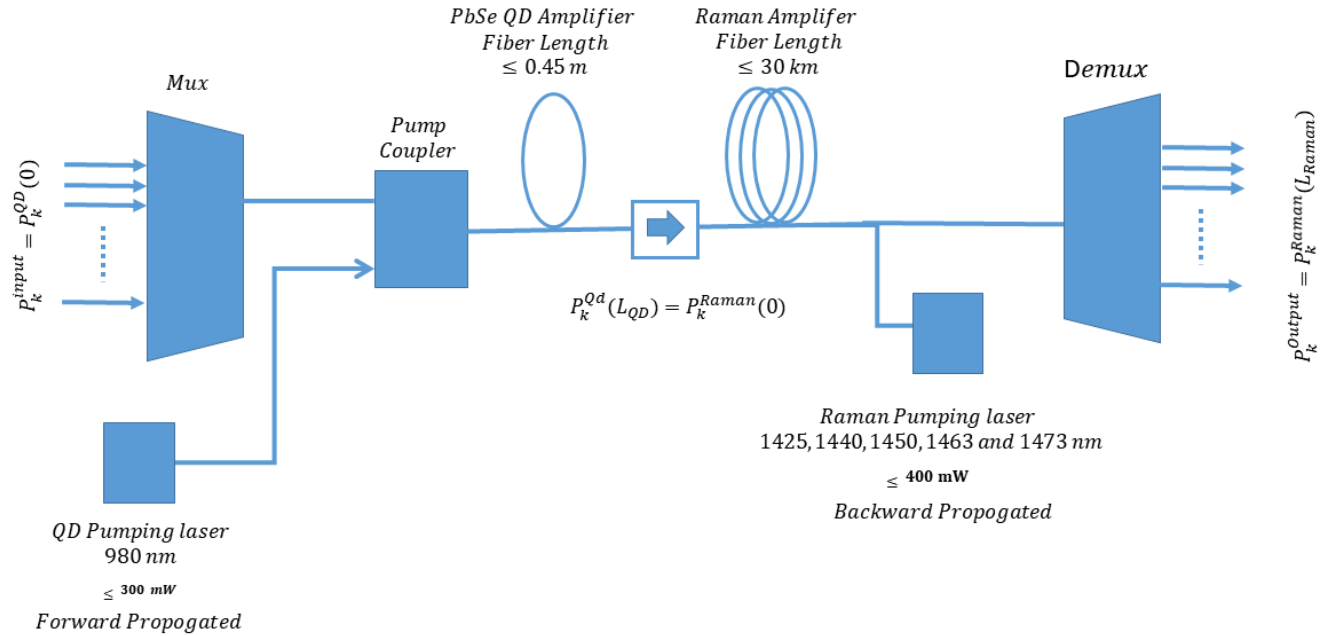

Fig. 1. The schematic diagram of the hybrid PbSe-QD/Raman amplifier used in the simulation

2. Modeling and equations

Fig. 1 shows the model used in our simulation for a PbSe-QD/Raman fiber amplifier, where the output power of PbSe-QD amplifier from the signal/noise $P_k^{QD}(L_{QD})$ is used as the input power for the Raman amplifier $P_k^{Raman}(0)$, where L_{QD} is the length of the PbSe-QD fiber. The input signal/noise for the k channel P_k^{input} is used as the input power for the signal/noise power of the PbSe-QD amplifier. The output signal for channel k is the same as the output of the Raman amplifier.

2.1. Quantum Dot Amplifiers

Our model of the quantum amplifiers is a three-level system as shown in Fig. 2, where the same model was used in Cheng et al. [20]. The rate equations for the ground state population n_1 and the excited-states populations n_2 and n_3 are given in Eq. (1-2), where $P_k(z)$ is the signal/Pump power of channel k with a frequency ν_k and bandwidth equal to $\Delta\nu_k$. σ_{ek} and σ_{ak} are the emission and absorption cross-section for channel k respectively, l_k represent the scattering attenuation cross-section, i_k is the transversal modal intensity, A_{21} is the non-radiative transition probability per unit time from level 2 to level 1, A_{32} is the non-radiative transition probability per unit time

from level 3 to level 2, and a represents the core radius. The first and second terms represent the stimulated emission due to the signal/pump powers and the noise respectively. Here, m=2 is used for the signal and amplified spontaneous emission (ASE) noise equation and m=0 for the pump power. The third term represents the absorption rate and the fourth term representing the attenuation due to scattering. We use the stationary state approximation where the time derivatives $\frac{dn_1}{dt} = 0, \frac{dn_2}{dt} = 0$ and $n1$ and $n2$ are solved from Eq. (1) and Eq. (2) as given below
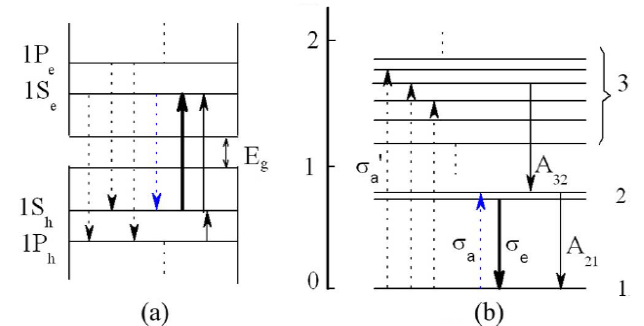

Fig. 2. The three-level diagram used to model the PbSe QD rate equations as found in Cheng et al [22] a) PbSe level diagram b) transition cross-section σ and decay lifetimes A (dotted lines denote absorption, bold solid lines represent radiative emission, and thin solid lines non-radiative emission)

$$\frac{dn_1}{dt} = -\sum_k \frac{P_k(z)i_k(r)\sigma_{ka}}{h\nu_k}n_1(r,z)$$

$$+\sum_k \frac{P_k(z)i_k(r)\sigma_{ke}}{h\nu_k}n_2(r,z)$$

$$+\frac{P_p(z)i_p(r)\sigma_{ep}}{h\nu_p}n_3(r,z)$$

$$+A_{21}n_2(r,z) \qquad (1)$$

$$\frac{dn_2}{dt} = \sum_k \frac{P_k(z)i_k(r)\sigma_{ka}}{h\nu_k}n_1(r,z) -$$

$$\sum_k \frac{P_k(z)i_k(r)\sigma_{ke}}{h\nu_k}n_2(r,z) - A_{21}n_2(r,z) + A_{32}n_3(r,z) \quad (2)$$

$$n_3 = n - n_2 - n_1 \qquad (3)$$

Their values are substituted in Eq. (3) and the power is solved numerically along the length of the fiber z where the rate equation for the power is

$$\frac{dP_k(z)}{dz}$$
$$= u_k\sigma_{ek}\int_0^a i_k(r)\,n_2(r)[P_k(z) + mh\nu_k\Delta\nu_k]2\pi r dr$$
$$- u_k\sigma_{ek}\int_0^a i_k(r)\,n_2(r)[P_k(z)]2\pi r dr$$
$$- l_k P(z) \qquad (4)$$

The parameters of PbSe-QD amplifier used in the simulation and their values are given in Table 1 and the normalized intensity for a single-mode fiber given by [1], [30]

$$i_k(r) = \frac{1}{\pi}\left[\frac{v_k}{av_k}\frac{j_0\left(\frac{u_k r}{a}\right)}{j_r(r)}\right]^2 \qquad (5)$$

where $j_0(r)$ and $j_1(r)$ are the Bessel functions, $V_k = 2\pi/\lambda_k(n_{core}^2 - n_{clad}^2)$ is the normalized frequency and u_k is found by matching the solution at $r = a$. Eq. (2) represents two rate equations for each channel. One equation represents the signal and noise and the other representing the rate equation for the pump power at 980 nm. We also assume a multi-quantum dot-doped amplifier consists of three different diameters of 5.5 nm ± 10%. The signal, noise and pump power are propagated by solving Eq. (4) numerically. The code is written in C language and Eq. (3) is solved numerically using GSL library implementation of the Prince-Dormand (8,9) algorithm [31], [32].

2.2. Raman Amplifiers

The rate equation for Raman amplifiers can be written as

$$\frac{dP_\nu^\pm}{dz} = \mp\alpha_\nu P^\pm \pm \epsilon_\nu P_\nu^\mp \pm P_\nu^\pm \sum_{\mu>\nu}\frac{g_{\mu\nu}}{\Gamma A_{eff}}\left(P_\mu^+ + P_\mu^-\right)$$

$$\pm 2h\nu\Delta\nu\sum_{\mu>\nu}\frac{g_{\mu\nu}}{\Gamma A_{eff}}\left(P_\mu^+ + P_\mu^-\right)(1$$

$$+ \eta(T))$$

$$\mp P_\nu^\pm \sum_{\mu<\nu}\frac{\omega_\nu}{\omega_\mu}\frac{g_{\mu\nu}}{\Gamma A_{eff}}\left(P_\mu^+ + P_\mu^-\right) \pm$$

$$4h\nu\Delta\nu\sum_{\mu<\nu}\frac{\omega_\nu}{\omega_\mu}\frac{g_{\mu\nu}}{\Gamma A_{eff}}\left(P_\mu^+ + P_\mu^-\right)(1 + \eta(T)) \qquad (6)$$

The ± symbols denote the forward and backward propagated powers. The first term represents the attenuation decay, the second term represents Rayleigh backward scattering, the third and fourth represent the power and ASE gain, and finally, the fifth terms represent the depletion in power due to stoke conversion. The gain efficiency of Raman fibers (AllWave, TrueWave, SMF, LEAF, Corning DZF and Corning NZDSF) are listed in Table 2. A modified version of the code authored by Jose Kraus Perin [33] is used in our simulation where the parameters, symbol and values for Eq. (6) used in this code are also given in Table 2. Here, we assume a multi-pumped Raman fiber that is pumped at the following wavelengths: 1425, 1440, 1450, 1465, and 1473 nm. The eq. (6) is solved using Matlab bv4pc function [34]. The output power for the signal and noise channel from the PbSe-QD amplifier is used as the input power for the Raman amplifier and the gain is calculated as

$$Gain(\lambda_k) = 10.0\log_{10}\frac{P_k^{Raman}(L_{Raman})}{P_k^{QD}(0)} \qquad (7)$$

where $P_k(0)$ is the signal input power at the PbSe-QD amplifier input and $P_k(L)$ is the power at the Raman fiber output. Denoting the Raman gain efficiency as Cr where the gain efficiency is defined as

$$C_r(\mu - \nu) = \frac{g_{\mu\nu}(\mu - \nu)}{\Gamma A_{eff}} \qquad (8)$$

We use the following form for the Raman efficiency

$$C_r = C_{peak}C_{normalized} \qquad (9)$$

where C_{peak} is the peak value for the Raman gain efficiency and $C_{normalized}$ is the normalized gain. The attenuation coefficient at different wavelengths for the different Raman fibers could be found in [10]. For the PbSe-QD amplifier, we assume that the fiber is co-doped with three different radii whose absorption and emission cross-sections are the same as those found in Cheng et al. [22]. Table 1 and Table 2 contain the parameters used in our simulation for the QD-PbSe amplifier and Raman amplifier respectively. It is also important to mention that for the PbSe-QD only amplifier, the input signal power goes through the PbSe-QD fiber first, and its output $P_k^{QD}(L_{QD})$ is used to calculate the gain for the PbSe only

amplifier as described in subsection 2.1. The same happens to the Raman only gain where the input signal propagates through the Raman fiber at the second stage shown in Fig. 1 and its output is used to calculate the gain as described in subsection 2.2.

3. Results and discussion

In this section, we represent the result of our simulation where for the PbSe-QD/Raman amplifier, the input power $P_k^{QD}(0)$ for both the signal and noise channels propagates through the PbSe-QD power first, and its output power is obtained by solving Eq. (1) to Eq. (4). This output is then used as input power for the Raman amplifier whose output power $P_k^{Raman}(L_{Raman})$ is obtained by solving Eq. (6). The gain is then calculated using Eq. (7). For the PbSe-QD only amplifier, the signal and noise propagate through the PbSe-QD fiber only and its output $P_k^{QD}(L_{QD})$ is used to calculate the gain in Eq. (7) replacing $P_k^{Raman}(L_{Raman})$. Table 3 shows the maximum gain values for the proposed hybrid PbSe-QD/Raman amplifier of several commercial Raman fiber at the default settings of PbSe-QD fiber length of 44 cm and pumping power of 300 mW, and the Raman fiber length of 30 km and the pumping power of 400 mW, compared to the Raman only and PbSe-QD only amplifiers of the same settings. From our observation, the Corning DSF has given the maximum gain in both hybrid and Raman amplifiers, compared to the rest of the Raman fibers. Table 4 shows the maximum gain obtained from the hybrid PbSe-QD/Raman of Corning DSF using the default settings compared to EDFA and EDFA/Raman amplifiers as given by Mahran et al [35]. From the table, our proposed hybrid amplifier has obtained a better maximum gain than the EDFA but it is still far to beat the gain obtained from EDFA/Raman amplifier.

3.1. The Gain Profile

We assume that the optimum fiber lengths for quantum doped fiber amplifier is 0.45 m, found by Cheng et al [22] and Raman amplifiers of 35 km. These values are taken as the default fiber length parameters. The PbSe-QD amplifier is pumped at 980 nm and 300 mW while the Raman amplifier is pumped at 400 mW for wavelengths 1425 nm, 1440 nm, 1450 nm, 1465 nm and 1473 nm as in Fig. 3 where in this figure, the calculated gain for the PbSe-QD amplifier only is obtained by solving Eq. (1) to Eq. (4). We use 100 channels each of width of 1 nm spanning a wavelength from 1525 nm to 1625 in this calculation.

3.2. Dependence on Raman Fiber Length

In Fig. 4 we show the dependence of the gain profile with the length of Raman optical fiber. The optical quantum dot amplifier is pumped at 980 nm at 300 mW and the Raman fiber is backward pumped at wavelengths at 1425 nm, 1440 nm, 1450 nm, 1465 nm, and 1473 nm with pumping power of 400 mW. The gain increases

significantly around 10 dB with the increase of the Raman fiber length by 20 km and the maximum rise is seen at wavelength of 1560 nm. The increase in gain with greater Raman fiber length could be explained by the rise of Stimulated Raman Scattering (SRS) signal amplification which is represented by the third term in Eq. (6) that increases with length as the signal propagates through the Raman fiber. The limiting behavior could be explained by the observation that almost all power of 400 mW is absorbed by the 20 km fiber. The SRS gain efficiency is reduced as the signal wavelength and pumping wavelength difference decreases, thus the attenuation which increases with increasing Raman fiber length dominates, and the gain is reduced as the signal wavelength becomes higher.
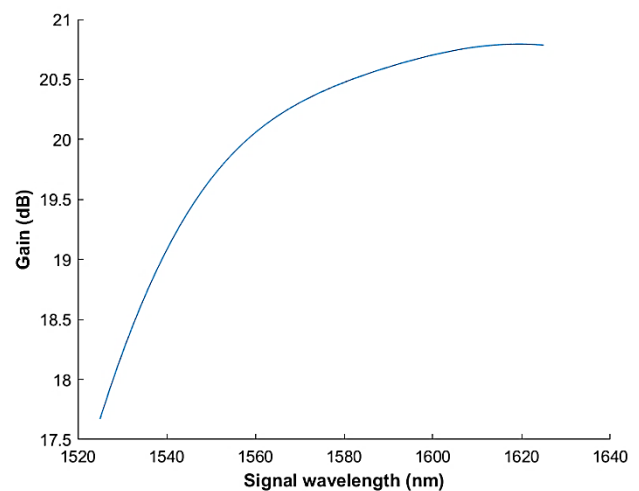

Fig. 3. Gain of 44 cm long PbSe-QD amplifier pumped at 980 nm at a power of 300 mW

3.3. Dependence on Raman Pumping Power

In Fig. 5, we show the dependence of the gain profile with the pumping power of Raman optical fiber. Here, the optical quantum dot amplifier is pumped at 980 nm at 300 mW and the Raman fiber is backward pumped at wavelengths at 1425 nm, 1440 nm, 1450 nm, 1465 nm and 1473 nm. A threshold of 200 W for the Raman pumping power is required to achieve higher gain. The gain is optimum at wavelength 1560 nm. The increase in gain with increasing Raman pumping power could also be explained by the increase in the (SRS) term amplification which increases signal amplification as the Raman pumping power increase.

3.4. Dependence on PbSe-QD Fiber Length

In Fig. 6, we show the dependence of the gain profile with the length of the PbSe-QD optical fiber. Here, the Raman fiber is backward pumped at wavelengths at 1425 nm, 1440 nm, 1450 nm, 1465 nm, and 1473 nm with pumping power of 400 mW and the optical quantum dot amplifier is pumped at a wavelength of 980 nm at 300 mW pumping power. We see that the gain increases with

increasing PbSe-QD fiber length reaching an optimum length at about 40 cm. This could also be explained by the Stimulated Emission Amplification (SEA) – represented by the first term in Eq. (4). This increase in gain by the ASE process increases the signal power as it propogates along the fiber from the pumping power. However, after a certain length of around 40 cm, where almost all of the the 300 mW pumping power is absorbed, almost no ASE gain is achived at lengths higher than 40 cm.

3.5. Dependence on PbS-QD Pumping Power

In Fig. 7, we show the dependence of the gain profile on the pumping power of the PbSe-QD amplifier fiber. Here, the optical quantum dot amplifier is pumped at 980 nm at a length of 44 cm and the Raman fiber is backward pumped at wavelengths of 1425 nm, 1440 nm, 1450 nm, 1465 nm, and 1473 nm at a power of 400 mW. The pumping power for the PbSe-QD fiber is increased from 50 mW to 300 mW in steps of 50 mW. We see that a 50 mW PbSe-QD pumping power increases the gain by around 10 dB, and it remains almost constant after that. The increase in the gain with PbSe-QD pumping power is due to the rise of signal power through SEA which increases the signal power as the pumping power becomes

higher, however, this SEA reaches a limiting behavior for a value of QD pumping power of around 150 mW.

Table 1. The parameters used in the PbSe-QD simulation

Parameter	Symbol	Value
Core radius	a	4.1×10^{-6} μm
Concentration of QD particles for each radius	N	1.0×10^{21} m^{-3}
Scattering attenuation coefficient	l_k	0.03 dB/m
Power Propagation direction sign	u_k	+ forward, - backward
Pumping power input	$P_p(0)$	Up to 300 mW
Pumping power Wavelength	λ_p	980 nm
Signal power input	$P_k(0)$	1.0×10^{-5}
Channel Bandwidth	Δλ	1 nm
Number of channels	N_{ch}	100
Minimum wavelength for the channel	λ_{min}	1525 nm

Table 2. The parameters used in the Raman amplifier simulation [10], [19]

Parameter	Symbol	Value
Absorption Coefficient	α_k	0.18 – 0.28 dB/km
Raman Gain Efficiency	C_p	Allwave 0.36 W^{-1}km^{-1} TrueWave RS 0.6 W^{-1}km^{-1} SMF 0.39 W^{-1}km^{-1} LEAF 0.46 W^{-1}km^{-1} CorningDSF 0.67 W^{-1}km^{-1} Corning NZDSF 0.72 W^{-1}km^{-1}
Rayleigh Backscattering	ϵ_k	60 dB km^{-1}
Pumping wavelengths	$\lambda_{p1}, \lambda_{p2}, \lambda_{p3}, \lambda_{p4}, \lambda_{p5}$	1425,1440,1450, 1465 and 1473 nm
Channel Bandwidth	Δλ	1 nm
Number of channels	N_{ch}	100
Minimum wavelength for the channel	λ_{min}	1525 nm

Table 3. Maximum gain comparison for hybrid PbSe-QD/Raman, Raman only, and PbSe-QD only amplifiers using several Raman fibers

Raman Fiber	Maximum gain (dB)		
	PbSe-QD/Raman	Raman only	PbSe-QD only
TrueWave	31.5	22.5	20.7
SMF	29.2	14.2	20.7
LEAF	30.2	17.2	20.7
Corning DSF	32.4	27.1	20.7
Corning NZDSF	31.9	24.7	20.7
ALLWAVE	28.6	12.7	20.7

Table 4. A comparison of maximum gain in hybrid PbSe-QD/Raman, EDFA/Raman and EDFA amplifiers

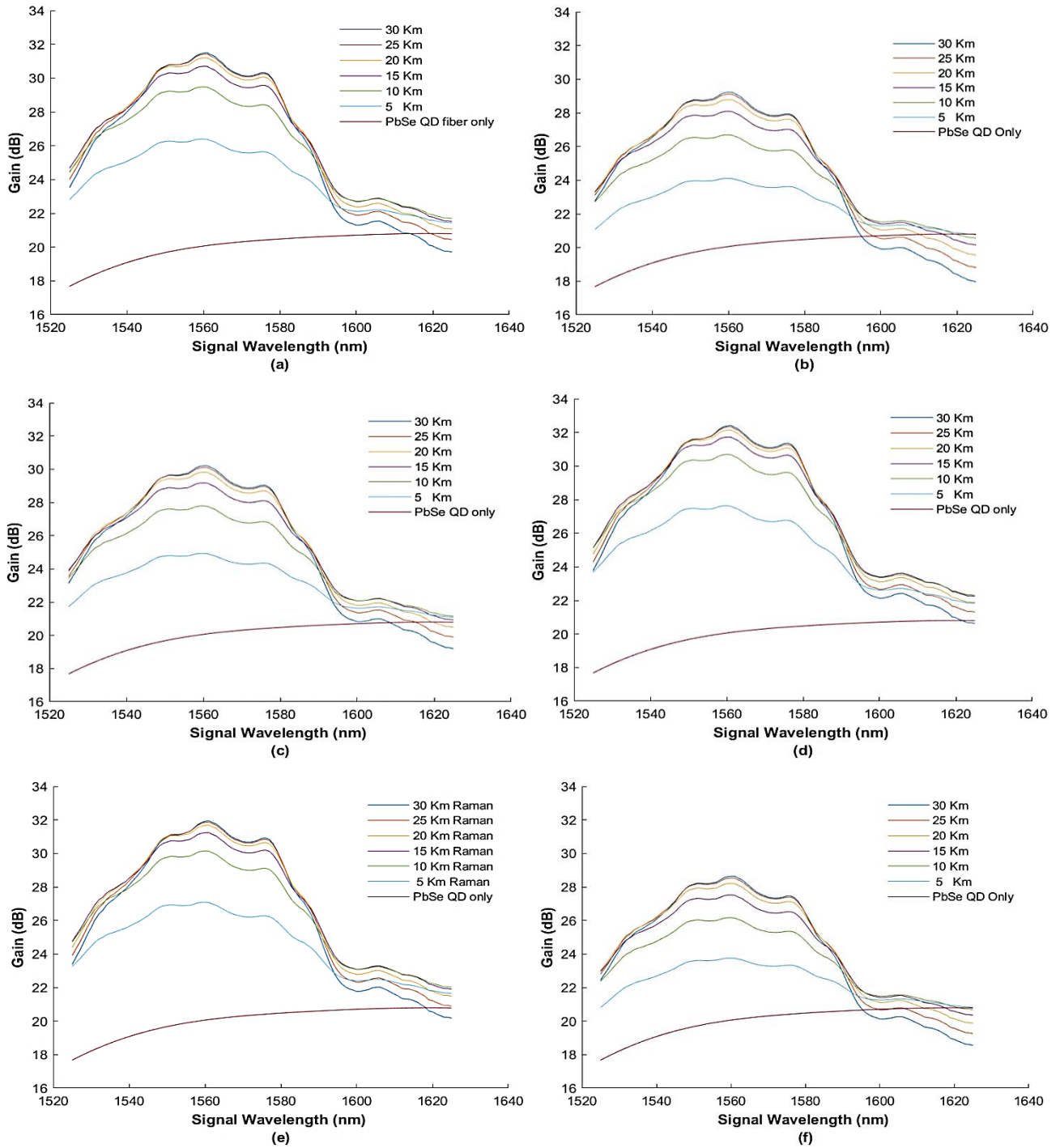| Amplifier	Maximum Gain (dB)
Hybrid PbSe-QD/Raman	32.4
EDFA/Raman	41.1
EDFA	24.3

Fig. 4. Hybrid amplifier gain dependence on Raman fiber length for (a)TrueWave RS (b) SMF (c) LEAF (d) Corning DSF, and (e) Corning NZDSF (f) AllWave fibers (color online)
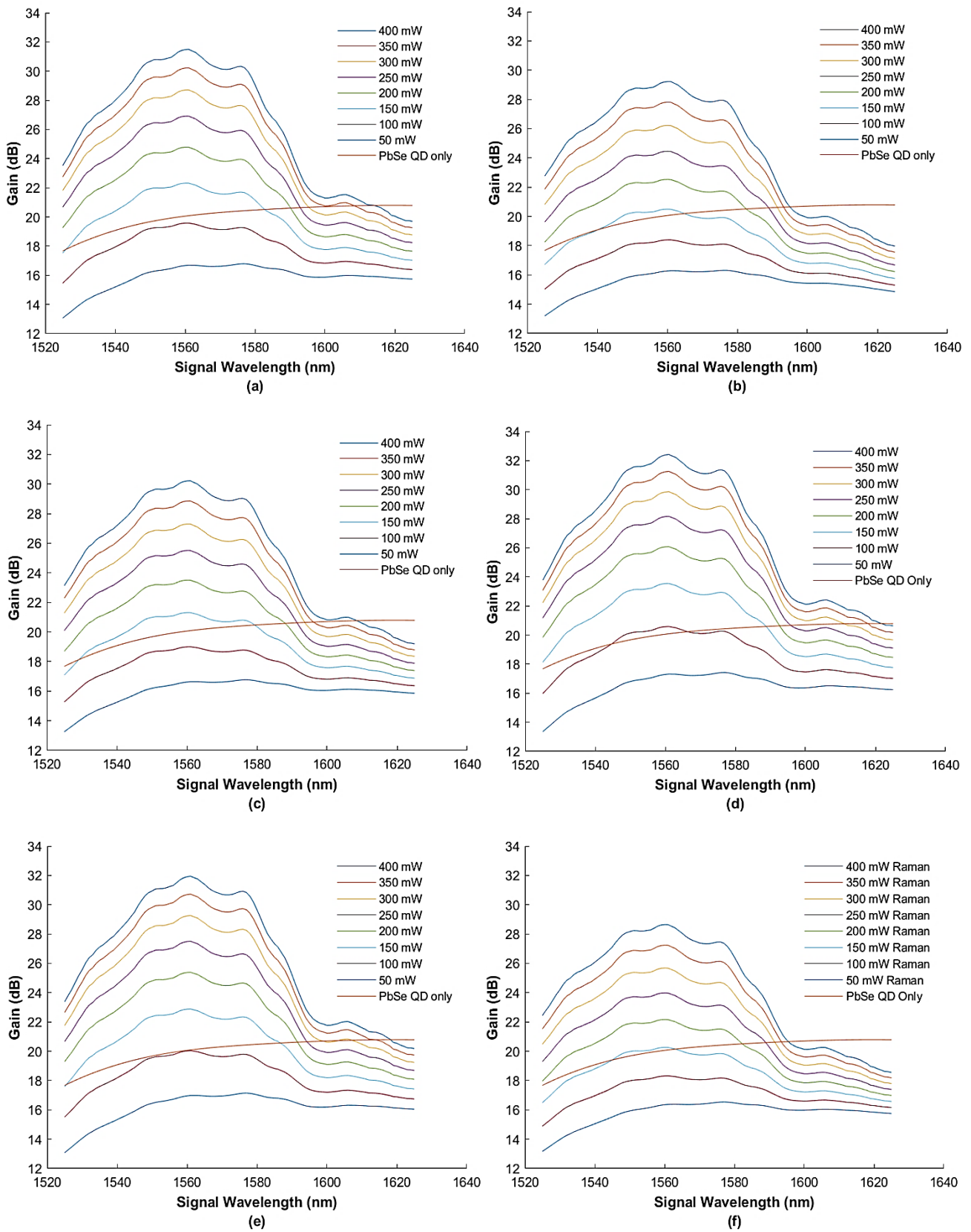
*Fig. 5. Hybrid amplifier gain dependence on Raman pumping power for (a) TrueWave RS (b) SMF (c) LEAF
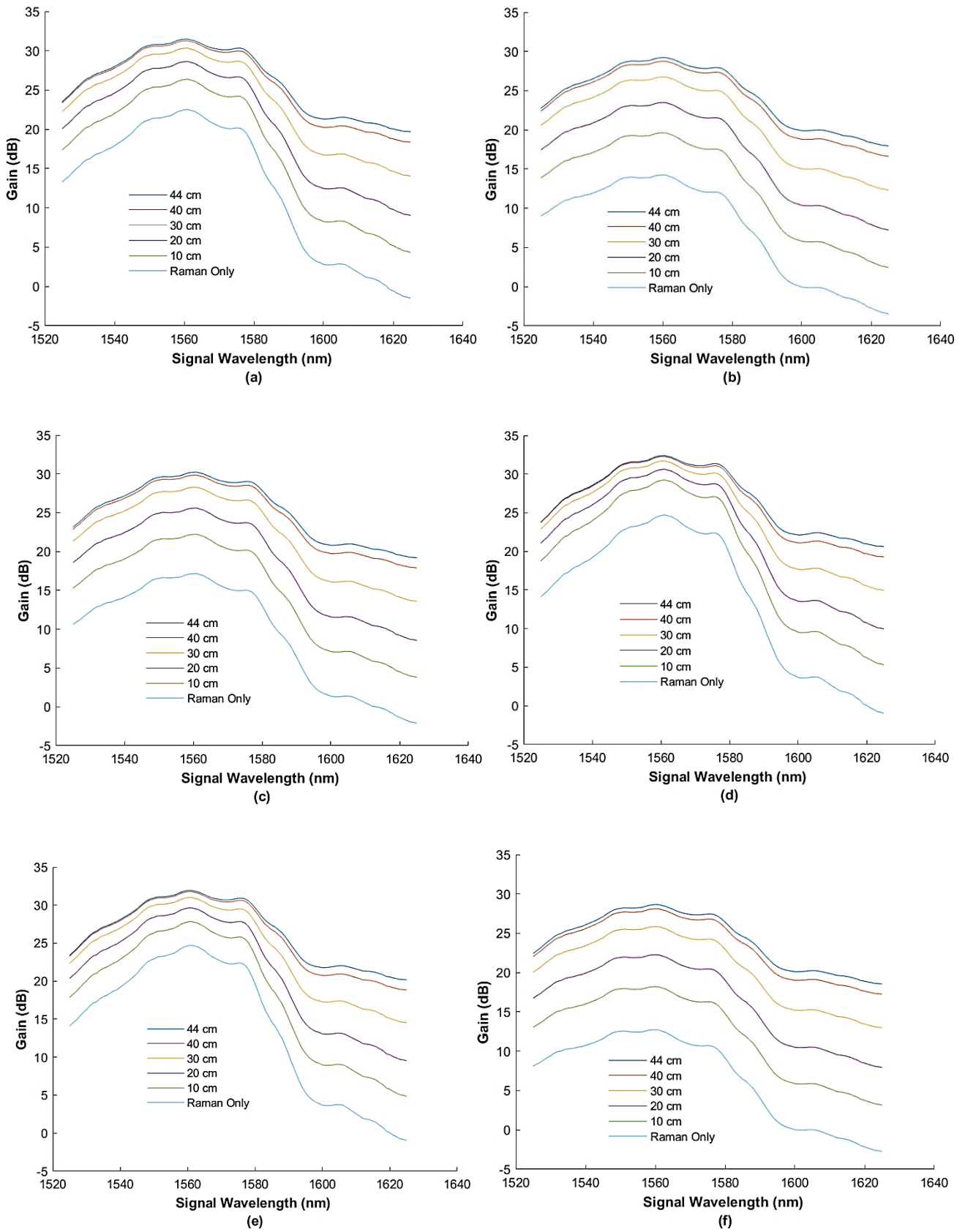(d) Corning DSF,(e) Corning NZDSF, and (f)AllWave fibers (color online)*

Fig. 6. Hybrid amplifier gain dependence on PbSe-QD fiber length for (a) TrueWave RS (b) SMF (c) LEAF (d) Corning DSF,(e) Corning NZDSF, and (f)AllWave fibers (color online)
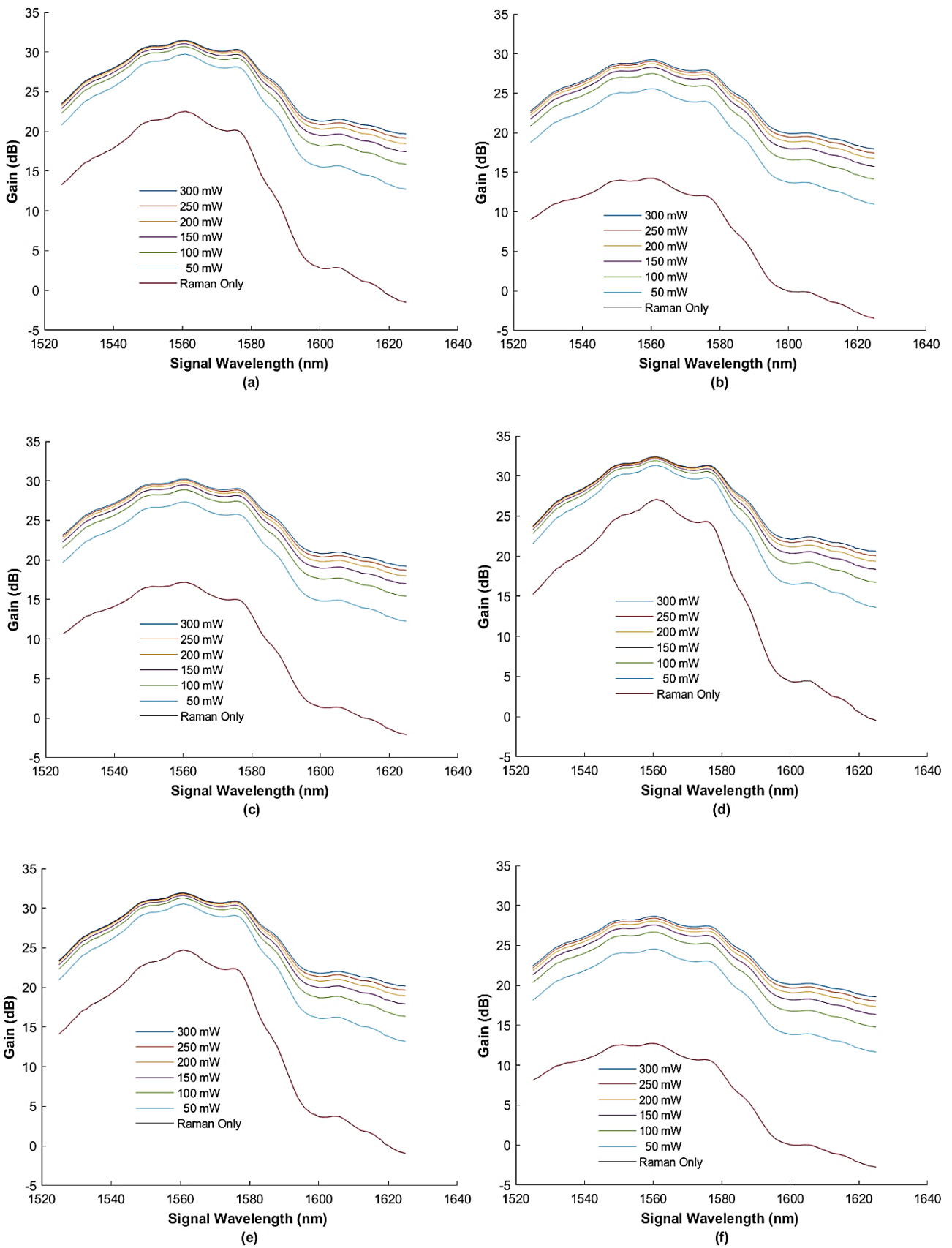
Fig. 7. Hybrid amplifier gain dependence on PbSe-QD pumping power for (a) TrueWave RS (b) SMF
(c) LEAF (d) Corning DSF,(e) Corning NZDSF, and (f)AllWave fibers (color online)

4. Conclusion

By changing the radius of the quantum dots, quantum dot optical amplifiers such as PbSe-QD provide desirable amplification characteristics over a wide range of wavelengths [36]. Raman optical amplification is also independent of the signal wavelength, thus a hybrid PbSe-QD/Raman amplifier would provide an optical hybrid amplifier over a wide range of wavelengths and highly tunable properties. In this paper, we study for the first time a proposed PbSe-QD/Raman amplifier through numerical modeling for several commercial Raman amplifiers. The proposed amplifier have gain dependence on both the PbSe-QD and Raman amplifiers lengths and pumping powers over the wavelengths spanning from 1525 nm to 1625 nm. We have used numerical modeling to achieve an accuracy that is greater than analytical approximations. It is shown that the hybrid amplifier has provided an improved gain compared to the two single amplifiers since the dependence on the length and pumping power of each amplifier provides limiting behavior. Compared to the EDFA/Raman amplifier, the proposed hybrid amplifier has lower gain values which is mainly due to the PbSe-QD scattering [37]. Further research is required to reach optimum values for the parameters under study.

References

[1] E. Desurvire, Erbium-doped fiber amplifiers : principles and applications. Wiley-Interscience, 2002.

[2] O. Mahran, A. E. El-Samahy, M. S. Helmy, M. A. el Hai, Optoelectron. Adv. Mat. **4**(12), 1994 (2010).

[3] L. Goldberg, J. Koplow, Electron. Lett. **34**(21), 2027 (1998).

[4] B. Sudhakar Reddy et al., Ceram. Int. **41**(3), 3684 (2015).

[5] S. V. Muravyev et al., Sci. Rep. **8**(1), 1 (2018).

[6] B. Zhou, H. Lin, D. Yang, E. Y.-B. Pun, Opt. Lett. **35**(2), 211 (2010).

[7] W. J. Chung, H. S. Seo, B. J. Park, J. T. Ahn, Y. G. Choi, ETRI J. **27**(4), 411 (2005).

[8] C. Headley, G. P. (Govind P. Agrawal, Raman amplification in fiber optical communication systems. Elsevier, 2005.

[9] R. H. Stolen, Fundamentals of Raman Amplification in Fibers, in Raman Amplifiers for Telecommunications 1, Springer New York, 2007, pp. 35–59.

[10] M. N. Islam, Raman Amplifiers for Telecommunications 1, Physical Principles, Springer, 2004.

[11] M. Rini, I. Cristiani, V. Degiorgio, A. S. Kurkov, V. M. Paramonov, Opt. Commun. **203**(1–2), 139 (2002).

[12] J. Chen, H. Jiang, IEEE Photonics J. **10**(2), 1 (2018).

[13] D. Zibar, A. Ferrari, V. Curri, A. Carena, "Machine Learning-Based Raman Amplifier Design," in 2019 Optical Fiber Communications Conference and Exhibition, OFC 2019 - Proceedings, Apr. 2019, p. M1J.1, doi: 10.1364/ofc.2019.m1j.1.

[14] C. J. A. Bastos-Filho et al., J. Microwaves, Optoelectron. Electromagn. Appl. **10**(2), 323 (2011).

[15] S. P. N. Cani, L. de Calazans Calmon, M. J. Pontes, M. R. N. Ribeiro, M. E. V. Segatto, A. V. T. Cartaxo, J. Light. Technol. **27**(7), 944 (2009).

[16] M. A. Iqbal, P. Harper, W. Forysiak, OSA Technical Digest (online) (Optical Society of America, 2018), paper NpTh1H.2. https://doi.org/10.1364/NP.2018.NpTh1H.2

[17] C. Cheng, S. Wang, X. Cheng, Opt. Laser Technol. **44**(5), 1298 (2012).

[18] M. Li, Y. Zheng, W. Liang, Y. Yuan, Y. Chai, R. Yuan, Chem. Commun. **52**(52), 8138 (2016).

[19] C. Y. Cho, C. W. Huang, Y. W. Lee, C. M. Chen, Proceedings - 2018 7th International Symposium on Next-Generation Electronics, ISNE 2018, Jun. 2018, pp. 1–3.

[20] C. Cheng, N. Hu, X. Cheng, Opt. Commun. **382**, 470 (2017).

[21] C. Cheng, H. Zhang, Opt. Commun. **277**(2), 372 (2007).

[22] C. Cheng, J. Light. Technol. **26**(11), 1404 (2008).

[23] A. R. Bahrampour, H. Rooholamini, L. Rahimi, A. A. Askari, Opt. Commun. **282**(22), 4449 (2009).

[24] O. Mahran, Opt. Commun. **353**, 158 (2015).

[25] O. Mahran, Opt. Mater. **52**, 100 (2016).

[26] S. Singh, R. S. Kaler, Opt. Laser Technol. **68**, 89 (2015).

[27] H. M. Obaid, H. Shahid, Optik **175**, 284 (2018).

[28] H. M. Obaid, H. Shahid, Optik **200**, 163404 (2020).

[29] N. M. Yusoff, A. H. Sulaiman, M. H. Al-Mansoori, M. A. Mahdi, Optik **210**, 164506 (2020).

[30] L. Kazovsky, S. Benedetto, A. E. Willner, Optical Fiber Communication Systems. Artech House, 1996.

[31] J. R. Dormand, P. J. Prince, J. Comput. Appl. Math. **6**(1), 19 (1980).

[32] P. J. Prince, J. R. Dormand, J. Comput. Appl. Math. **7**(1), 67 (1981).

[33] J. K. Perin, "GitHub - jkperin/raman-amplifiers: Design and analysis of Raman optical amplifiers." https://github.com/jkperin/raman-amplifiers (accessed Jan. 08, 2021).

[34] J. Kierzenka, L. F. Shampine, ACM Trans. Math. Softw. **27**(3), 299 (2001).

[35] O. Mahran, A. Elsamahy, M. Aly, M. Abd, S. Arabia, Optoelectron. Adv. Mat. **9**(5-6), 575 (2015).

[36] C. Cheng, F. Wang, X. Cheng, Opt. Laser Technol. **122**, 105812 (2020).

[37] H. Du et al., Nano Lett. **2**(11), 1321 (2002).

*Corresponding author: hassan.yossry_PG@alexu.edu.eg